Kinetic study of 1-butanol dehydration to di-n-butyl ether over Amberlyst 70

M. A. Pérez-Maciá, R. Bringué, M. Iborra, J. Tejero and F. Cunill

Department of Chemical Engineering, University of Barcelona, C/Martí i Franquès, 1, 08028 – Barcelona

Abstract

Kinetics of the catalytic dehydration of 1-butanol to di-n-butyl ether (DNBE) over Amberlyst-70 was investigated. Experiments were performed in liquid phase at 4 MPa and 413-463 K. Three elementary reaction mechanisms were considered: a Langmuir-Hinselwood-Hougen-Watson (LHHW) formulation; an Eley-Rideal (ER) formulation in which DNBE remains adsorbed; an ER formulation in which water remains adsorbed.

Two kinetic models explain satisfactorily the dehydration of 1-butanol to DNBE: a LHHW formalism in which the surface reaction between two adjacent adsorbed molecules of 1-butanol is the rate limiting step (RLS) and where the adsorption of water is negligible, and a mechanism in which the RLS is the desorption of water being the adsorption of DNBE negligible. In both models the strong inhibiting effect of water was successfully taken into account by means of a correction factor derived from a Freundlich adsorption isotherm. Both models present similar values of apparent activation energies (122±2 kJ/mol).

Topical area: Reaction Engineering, Kinetics and Catalysis

Key words: di-n-butyl ether, 1-butanol, Amberlyst 70, kinetics, water inhibiting effect.

Introduction

Environmental regulations imposed over the past decades concerning diesel quality and vehicles emission have led to an active search for more efficient and cleaner fuels. In this search, di-n-butyl ether (DNBE) has been identified as an important candidate biofuel which can be produced from lignocellulosic biomass.[1,2] Besides the significant advantages of using lignocellulosic biomass as raw material (residues from agriculture, energy crops and forest refuse are produced in abundance and worldwide and they have no direct competition with food, thus being an attractive, inexpensive, renewable resource for the production of next generation of biofuels), DNBE presents excellent properties to be blended with diesel fuel[3]: it has a particularly high cetane number (100) indicating short ignition delay times which at the end translates into relatively longer combustion process and thus less unburned hydrocarbons; its moderate boiling point (415.6 K) allows facile vaporization of the fuel after engine injection while minimizing the volatile organic compounds emissions during storage, transport and refueling; finally, its volumetric energy content is comparable to that of petroleum fuels providing satisfactory engine power without modification of existing diesel engines.

Biobutanol can be produced from biomass either by fermentation or by thermochemical routes.[4,5] Currently, biobutanol is being produced on industrial scale through the ABE fermentation process in which biomass fermentation by microorganisms of the genus Clostridium gives place to 1-butanol along with acetone and ethanol.[6] Subsequently, DNBE can be obtained by dehydration of 1-butanol over acid catalysts.[7,8] In a previous work[9] it was showed that acidic ion-exchange resins were excellent catalysts for the selective dehydration of 1-butanol to di-n-butyl ether in liquid phase. Among the ion exchangers tested, Amberlyst 70 was selected as the most appropriate resin for industrial use due to its thermal stability (up to 463 K), its high selectivity to DNBE and its suitable activity.

In order to design and model an heterogeneous catalyzed process obtaining a reliable reaction rate expression is essential. From the few kinetic studies on 1-butanol dehydration, the majority have been carried out at experimental conditions in which butenes (resulting from 1-butanol intramolecular dehydration) are the main products.[10] Olaofe and Yue[10] studied the

kinetics of 1-butanol dehydration over three types of zeolites in gas phase in the temperature range 473 – 573 K and 1-butanol pressures up to 60 kPa. At these conditions the main products were both butenes and DNBE. For the dehydration of 1-butanol to di-n-butyl ether they considered a power law kinetic model as well as three Hougen-Watson type kinetic expressions assuming the surface reaction as the rate controlling step and that the adsorption of water and ether was negligible against the adsorption of 1-butanol. They concluded that empirical power functions rate expressions satisfactorily correlated the reaction rate data of the dehydration of 1-butanol to DNBE and found an activation energy of 54 – 142 kJ/mol (depending on the used zeolite). Krampera and Beránek[11] studied the kinetics of individual reactions for the dehydration of 1-butanol over alumina in gas phase at 433 K. For di-n-butyl ether formation they proposed a LHHW mechanism where the irreversible surface reaction of two adsorbed molecules of 1-butanol was the rate limiting step and assuming the adsorption of water and ether negligible against the adsorption of 1-butanol. Sow et al.[12] studied the kinetics of 1-butanol dehydration to DNBE in liquid phase (at 433, 453 and 473 K under autogenerated pressure) over three sulfonated mesoporous silica and organosilica catalyst and a Y-zeolite. In their study they only considered a kinetic rate expression based on a mechanism where one molecule of 1-butanol adsorbs on an active site, the irreversible surface reaction being the rate limiting step and assuming the adsorption of alcohol and ether to be negligible against the adsorption of water, $r = k \cdot [DNBE] / \left(1 + K_{H_2O} [H_2O]\right)$. The values of the activation energies that they obtained ranged between 95 – 97 kJ/mol.

The main goal of this study was to perform a comprehensive kinetic analysis of DNBE synthesis on the acidic resin Amberlyst 70 in the liquid phase at the temperature range of 413 – 473 K. Particular emphasis was placed on high water contents given its inhibitory effect.[13-16]

Experimental

Material

1-butanol (≥ 99.4 w/w % pure; ≤ 0.1 w/w % butyl ether; ≤ 0.1 w/w % water) and DNBE (≥ 99.0 w/w % pure; ≤ 0.05 w/w % water) supplied by Acros Organics were used without further purification. Deionised water (resistivity 18.2 mΩ·cm) obtained in our laboratory and N_2 (≥ 99.995 w/w %) supplied by Abelló Linde were also used.

The macroreticular thermostable resin Amberlyst-70 supplied by Rohm and Haas was used as the catalyst. Amberlyst-70 is a low cross-linked chlorinated and sulfonated copolymer of styrene-divinylbenzene (S-DVB), stable up to 463 K. Its acid capacity, determined following the procedure described by Fisher and Kunin[17], was found to be 2.65 mol H^+/kg. Table 1 gathers the main properties of Amberlyst 70.

Apparatus and analysis

Experiments were carried out in a 100 cm^3 316 stainless steel autoclave (Autoclave Engineers, M010SS, maximum temperature: 505 K; pressure range: 0 – 15 MPa).

The system was equipped with a pneumatic injection system to load the catalyst, a magnetic drive stirrer and a 400 W electrical furnace for heating. Temperature and stirring speed were measured by a thermocouple located inside the reactor and by a tachometer. Both operation variables were controlled to ± 1 K and ±1 rpm respectively by an electronic control unit. One of the outlets of the reactor was connected directly to a liquid sampling valve, which injected 0.2 mm^3 of pressurized liquid into a gas-liquid chromatograph equipped with a TCD detector (Agilent Technologies, 7820A). Analysis procedure is described in detail elsewhere.[9]

Procedure

Wet resin (as provided by the supplier) was dried at room temperature for 24 h prior to mechanical sieving. Afterwards, resin samples with bead size between 0.40 – 0.63 mm were dried at 383 K in an atmospheric oven during 3 h and then under vacuum (1 kPa) for 15 h. A previous work showed that after this drying treatment the residual water content of the resin was <3% (w/w).[18] 70 mL of 1-butanol, or 1-butanol/water, or 1-butanol/DNBE were charged in the reactor and heated to the working temperature. The pressure was kept at 4 MPa with N_2 to

ensure that the reaction medium was in liquid phase over the whole temperature range and the stirring speed was set at the corresponding value (300-700 rpm). Once the corresponding working temperature was reached (413-163K), the dried catalyst was injected by means of pneumatic transport considering this time as the starting point of reaction. Liquid composition was analyzed hourly during 7 h.

Reaction rates of DNBE formation were obtained from the function of the DNBE moles produced vs. time (Equation 1). A rational function was used to describe the relationship between n_{DNBE} and t.

$$r_{DNBE}(t) = \frac{1}{W_{cat}}\left(\frac{dn_{DNBE}}{dt}\right) \qquad \left[\frac{mol}{h \cdot kg_{cat}}\right] \qquad (1)$$

Measured reaction rate were accurate within ± 5%

Results and Discussion

Preliminary experiments

In order to check that the overall observed reaction rates were not influenced by mass transfer limitations or solid distribution effects, a set of preliminary experiments was conducted by changing the resin particle size, stirring speed and the catalyst loading of the reactor. Since external mass transfer depends both on particle size and stirring speed, instead of three series of experiments in which, one by one, the effect of particle size, stirring speed and catalyst loading was tested, a factorial design of experiments[19] was carried out, since it allows to study the simultaneous effect of the three factors (stirring speed, N; catalyst particle size, d_p; mass of loaded catalyst, W_{cat}). Each factor was studied at two levels, i.e. following a 2^3 factorial design. Taking into account the operation conditions in which the dehydration reactions of 1-pentanol and 1-octanol to linear ether over Amberlyst 70 were not influenced by mass transfer limitations[20,21], the following range for the three factors was selected: (catalyst mass: 0.5-2 g; stirring speed: 300-700 rpm; catalyst particle size: 0.4-0.8 mm). Table 2 shows the experimental matrix for the 2^3 factorial design. Some of the eight formulations (denoted with an *) were replicated and four additional runs (last 4 rows) were carried out at the central point of the

design (500 rpm, 1g of catalyst with particle size between 0.4-0.63 mm). The last column in Table 2 shows the initial rate of DNBE formation obtained for each run. The order in which the runs were carried out was randomized to avoid systematic errors. All tests were performed at 4 MPa and at the highest temperature of the range explored, which corresponds to the catalyst maximum operating temperature (463 K).

As can be seen in Table 2, reaction rates measured in all the experiments are quite close; most of them can be taken as the same within the limits of the experimental error. In order to examine statistically the influence of the studied factors on the reaction rate, a linear regression model (Equation 2) which considered as regressor variables the main effects (N, d_p, W_{cat}) as well as the interaction effects ($N \cdot d_p$; $N \cdot W_{cat}$; $d_p \cdot W_{cat}$; $N \cdot d_p \cdot W_{cat}$) was fitted to data of Table 2 by the least squares method.

$$r^0 = 150.93 + 1.235 \cdot (N) + 2.445 \cdot (W_{cat}) - 4.051 \cdot (d_p) - 0.472 \cdot (N \cdot W_{cat}) - 0.341 \cdot (N \cdot d_p) - 2.271 \cdot (W_{cat} \cdot d_p) - 0.677 \cdot (N \cdot W_{cat} \cdot d_p) \quad (2)$$

To evaluate whether Equation 2 represented the experimental data satisfactorily from a statistical standpoint, a *Test for the lack of fit*[22] was performed. By computing the variance due to pure error (s^2_{PE}) and the variance due to the lack of fit (s^2_{LOF}) it was possible to compare the test statistic $F_0 = s^2_{LOF} / s^2_{PE} = 0.868$ with the critical value of the $F_{distribution} = 4.737$ to ascertain if both variances were statistically different. It can be seen that $F_0 < F_{distribution}$ for a probability of 0.95. Thus, Equation 2 represents satisfactorily reaction rate data.

To determine whether the regressor variables contributed significantly to the model a *Test for significance of regression*[22] was performed. The test procedure involves computing the statistic F_0 as the ratio between the variance due to the regression, s^2_R, and the variance due to the experimental error, s^2_E, and compare this value with the critical value of the $F_{distribution}$. From the results of the test for significance it can be concluded that $F_0 = 2.608 < F_{distribution} = 3.293$ (for a probability of 0.95). Thus, none of the regressor variables contributed significantly to Equation 2. As a result, reaction rate values can be considered the same in the whole range of operation variables checked (N = 300 – 700 rpm, d_p = 0.4 – 0.8 mm and W_{cat} = 0.5 – 2 g).

Therefore, to carry out the kinetic experiments the following operation conditions were selected: N = 500 rpm, W_{cat} = 1 g of Amberlyst-70 and d_p = 0.4 – 0.63 mm.

Modeling of kinetic data

The reaction rate models considered in this work are based on the Langmuir-Hinshelwood-Hougen-Watson (LHHW) and the Eley Rideal (ER) formalisms. These formalisms, as well as the kinetic expressions derived from different rate limiting step (RLS) and quasi-steady states assumptions are discussed next.

Mechanism 1: Langmuir-Hinshelwood-Hougen-Watson (LHHW) formalism.

In the LHHW mechanism two alcohol molecules, each one adsorbed on an adjacent active site, react to yield the ether. The elementary steps for this model are shown in the following expressions, in which σ represents an active site and BuOHσ, DNBEσ and H_2Oσ correspond, respectively, to 1-butanol, di-n-butyl ether and water chemisorbed on an only active site.

$$BuOH + \sigma \xrightleftharpoons{K_{BuOH}} BuOH\sigma$$

$$2\ BuOH\sigma + n(\sigma) \xrightleftharpoons{K_s} DNBE\sigma + H_2O\sigma + n(\sigma)$$

$$DNBE\sigma \xrightleftharpoons{1/K_{DNBE}} DNBE + \sigma$$

$$H_2O\sigma \xrightleftharpoons{1/K_{H_2O}} H_2O + \sigma$$

Mechanism 2: Eley Rideal formalism where DNBE remains adsorbed (ER_{DNBE})

The ER formalism assumes that only one of the two reacting molecules of 1-butanol adsorbs on the surface and reacts with other one directly from the bulk yielding DNBE and water. The formed DNBE molecule remains adsorbed on the surface while water is immediately released into solution:

$$BuOH + \sigma \xrightleftharpoons{K_{BuOH}} BuOH\sigma$$

$$BuOH + BuOH\sigma + n(\sigma) \xrightleftharpoons{K_s} DNBE\sigma + H_2O + n(\sigma)$$

$$DNBE\sigma \xrightleftharpoons{1/K_{DNBE}} DNBE + \sigma$$

Mechanism 3: Eley Rideal formalism where water remains adsorbed (ER_{H2O})

As in mechanism 2, 1-butanol from solution reacts directly with 1-butanol adsorbed on the surface of the catalyst but, in this case, the ether is immediately released to the liquid phase and water remains adsorbed:

$$BuOH + \sigma \xrightleftharpoons{K_{BuOH}} BuOH\sigma$$

$$BuOH + BuOH\sigma + n(\sigma) \xrightleftharpoons{K_S} DNBE + H_2O\sigma + n(\sigma)$$

$$H_2O\sigma \xrightleftharpoons{1/K_{H_2O}} H_2O + \sigma$$

In the three mechanisms it was taken into account the possibility that *n* additional active sites (with *n* = 0, 1 or 2) could participate in the surface reaction.

Each of the elementary steps that take part in the reaction mechanisms just described can be considered as the rate limiting step. If the chemical reaction rate on the surface is considered the RLS, it is assumed that adsorption of species is maintained in a quasi-equilibrium state all the time. On the contrary, if the RLS is considered to be the adsorption of the reactant or the desorption of a product, it is assumed that the chemical reaction between adsorbed species is in quasi-equilibrium. Table 3 gathers the kinetic models derived from the three reaction mechanisms depending on the elementary step that is considered as the RLS. $\hat{k}$ is the forward rate constant for the surface reaction; k_j and K_j are, respectively, the adsorption rate constant and the adsorption equilibrium constant of compound *j;* K_{eq} is the thermodynamic equilibrium constant which was experimentally determined in a previous work.[23] All the rate expressions of Table 3 may be expressed as a combination of three terms, the kinetic, the driving potential and the adsorption term[24,25]:

$$r_{DNBE} = \frac{\text{kinetic term} \cdot (\text{driving potential term})}{(\text{adsorption term})^m} \qquad (3)$$

When the surface reaction is considered the RLS, the kinetic term is the product of the surface reaction rate constant for the forward reaction and a power of the 1-butanol adsorption equilibrium constant which depends on the considered mechanism. If the adsorption of 1-butanol or the desorption of one of the products is the RLS, the kinetic term is the rate constant

of the rate limiting adsorption/desorption process. The driving potential term accounts, in all rate expressions, for how far the thermodynamic equilibrium is, and it must become zero when the equilibrium is reached. Finally, the adsorption term accounts for all the species that are adsorbed on surface sites. The exponent on the adsorption term for the cases where the surface reaction is considered the RLS is equal to the number of active sites participating in the surface reaction. When the adsorption/desorption of a single species is the RLS, the corresponding element in the adsorption term is modified according to the surface reaction involved.

Simplified kinetic models were derived from the general kinetic models of Table 3 by assuming the amount of free active sites very low compared with the occupied ones (thus the unity present in the adsorption term can be removed), and/or the adsorption of alcohol, ether and/or water to be negligible. This way, 82 different kinetic models were obtained which have been included in the Supplementary Data section.

All the models where fitted to reaction rate data by minimizing the sum of squared relative errors (SSRE, Equation 4) using the Levenberg-Marquardt algorithm[26,27] which is implemented in Matlab. We consider the relative error to be a more meaningful measure[28,29] than the sum of squared errors, SSE ($SSE = \sum (r_{exp} - r_{cal})^2$), given that the range of rate values is large ($r_{DNBE} \approx$ 2 – 135 mol/h·kg).

$$SSRE = \sum \left(\frac{r_{exp} - r_{cal}}{r_{exp}} \right)^2 \qquad (4)$$

The dependence of the kinetic parameters with the temperature was considered to follow the Arrhenius law (Equation 5) for the rate constants ($\hat{k}$ and k_j), and the Van't Hoff law (Equation 6) for the adsorption equilibrium constants (K_j). Both expressions were reparameterized in order to avoid strong binary correlation between parameters.[30] T_{ref} is defined as the midpoint T value in the analyzed range of temperatures.

$$\hat{k}, k_j = A \exp\left[-\frac{E_A}{R} \left(\frac{1}{T} - \frac{1}{T_{ref}} \right) \right] \qquad (5)$$

$$K_j = \exp\left[\frac{\Delta S_j}{R} - \frac{\Delta H_j}{R}\left(\frac{1}{T} - \frac{1}{T_{ref}}\right)\right] \qquad (6)$$

The temperature dependence of the thermodynamic equilibrium constant was found to be[23]:

$$K_{eq} = \exp\left[\frac{37.0}{T} + 3.2\right] \qquad (7)$$

Whenever possible, rate and adsorption constants were grouped for mathematical fitting purposes. Equations 8-11 show, by way of example, how the constants association was done for the kinetic model LHHW-RLS2/1b (see Supplementary Data) which stemmed from the LHHW formalism when the following assumptions were made: (1) the surface reaction was considered the RLS; (2) the number of active center participating in the reaction was 3 and; (3) the amount of free active sites was very low compared with the occupied ones.

$$r_{DNBE} = \frac{k^* \cdot \left(a_{BuOH}^2 - \frac{a_{DNBE} \cdot a_{H_2O}}{K_{eq}}\right)}{\left(a_{BuOH} + K_1 \cdot a_{DNBE} + K_2 \cdot a_{H_2O}\right)^3} \qquad (8)$$

With

$$k^* = \hat{k} \cdot \frac{K_{BuOH}^2}{K_{BuOH}^3} = \hat{k} \cdot K_{BuOH}^{-1} \qquad (9)$$

$$K_1 = \frac{K_{DNBE}}{K_{BuOH}} \qquad (10)$$

$$K_2 = \frac{K_{H_2O}}{K_{BuOH}} \qquad (11)$$

Experiments starting from pure 1-butanol

A series of experiments with pure 1-butanol was conducted in the temperature range 413 - 463 K. Each experiment was, at least, duplicated (being the relative error corresponding to DNBE formation rates lower than 5%). Figures 1a and b represent, respectively, 1-butanol conversion and selectivity to di-n-butyl ether as a function of the reaction time for all the temperatures tested. From Figure 1a it could be concluded that 1-butanol normalized conversion

is strongly influenced by reaction temperature increasing from a value of 4% at 413 K to more than a tenfold (≈ 46%) at 463 K (after 7 h of experiment). However, it must be taken into account that the system is far away from the equilibrium position. In a previous work we found that the dehydration of 1-butanol to DNBE is a slightly exothermic reaction (almost athermic). Thus it is expected that, with time, the curves of conversion for all the tested temperatures tend to a very close value (not exactly the same value due to the existence of secondary reactions which are influenced by the temperature reaction).

Selectivity to DNBE also depends on the reaction temperature although in all cases was higher than 90%. As it can be seen, after some time selectivity reaches a plateau. The time needed to reach this plateau and the value to which the selectivity tends depends on the operating temperature: a higher reaction temperature results in longer times to reach a constant value (in experiments run at the higher temperatures, 443 – 463 K, selectivity was still moderately decreasing after 7 h) and lower selectivity to DNBE, other detected products being butenes, 2-butanol and the branched ether 1-(1-methylpropoxy)butane (a detailed scheme of the reaction network can be found elsewhere9). Nevertheless, for all the tested temperatures the catalyst is very selective to the linear ether.

Figure 1c shows the reaction rate of DNBE synthesis along the experiments as a function of temperature. As expected, the initial reaction rate is highly dependent on temperature doubling its value with each 10 K rise. However, reaction rate decreases along time (more sharply when the reaction temperature is high) and after 7 h the reaction rate for all the tested temperatures is very similar with values in the range of 2.3 - 11.1 mol/h·kg. This decrease could be due to an inhibition effect caused by the reaction products (it is well known that water adsorbs strongly on acidic sites influencing the reaction rate[13-16]).

Given the important dissimilarity between the compounds presents in the medium, the system deviates from ideality. In order to take into account this non-ideality, the kinetic analysis was carried out as a function of activities instead of concentrations. The activity coefficients were estimated by the UNIFAC-Dortmund predictive method.[31-34]

Figure 2 shows the dependence of the reaction rate as a function of activities of 1-butanol (a_{BuOH}), water (a_{H2O}) and di-n-butyl ether (a_{DNBE}). Due to the fact that a_{BuOH}, a_{H2O} and a_{DNBE} are not independent variables, it is difficult to analyze the influence that each activity has on the reaction rate. However, from Figure 2 it can be concluded that a decrease in $a_{BuOH,}$ which is associated with an increase in a_{H2O} and a_{DNBE}, affects negatively the DNBE reaction rate for all the temperatures tested.

General (Table 3) and simplified models (see Supplementary Data) were fitted to experimental data corresponding to runs starting from pure 1-butanol. Several kinetic models with physicochemical meaning (positive activation energy, negative adsorption enthalpy and negative adsorption entropy) fitted the experimental data satisfactorily. Models, fitted parameters, confidence intervals for a 95% probability, sum of squared relative errors and goodness of the fit (R^2_{adj}) for the best kinetic models are gathered in Table 4. Among these models, LHHW-RLS4/1b (Equation 13) and LHHW-RLS3/1b (Equation 14) present the lowest sum of squared relative errors (SSRE) and the lowest parameters uncertainty Δ (calculated with Equation 12, with ε_i being the uncertainty of parameter β_i and p de number of parameters in the model). Both equations stem from a LHHW formalism in which the rate limiting step is considered to be the desorption of one of the products (water and ether respectively) and assuming the amount of free active sites to be negligible in comparison with the other adsorption terms. On the other hand, model LHHW-RLS2/1b (Equation 15) stems from a LHHW formalism where the surface reaction is considered the rate limiting step. However, this model presents higher SSRE and parameters uncertainties significantly high.

$$\Delta=\left[\sum_{i=1}^{p}\left(\frac{\varepsilon_i}{\beta_i}\right)^2\right]^{0.5} \quad (12)$$

It must be pointed out that the concentration of alcohol, ether and water in the reaction medium are not independent variables, thus a_{BuOH}, a_{DNBE} and a_{H2O} are reciprocally dependent. Figure 3 shows the relation between water and DNBE activity. As it can be seen, the ratio a_{H2O}/a_{DNBE} is almost constant along the experiments for all the temperatures tested (except for

time = 0) with values ranging between 1.3 and 1.8, belonging the highest ratios to the highest temperatures. This tendency is in accordance with the lower selectivity observed for higher temperatures being water also produced through side-reactions. The significant high ratios observed at time = 0 h are probably due to residual water in the dry catalyst or in the reactant. Due to the fact that the ratio a_{H2O}/a_{DNBE} is almost constant, models LHHW-RLS4/1b (Equation 13) and LHHW-RLS3/1b (Equation 14) are equivalent. Similarity between fitted parameters of both models (Table 4) corroborates it. This fact makes impossible to differentiate, from this set of experiments, which of the two mechanisms prevails.

Distribution of residual of fitted models gathered in Table 4 must also be taken into account. As it can be seen in Figure 4a the model fits the experimental data satisfactorily. However, residuals do not show a random distribution. From Figure 4b it can be concluded that residuals corresponding to experiments performed at 463 K account significantly in the total sum of residuals. Data shown in Figure 4 corresponds to model LHHW-RLS4/1b (Equation 13) but for the rest of models gathered in Table 4 the trends are very similar. Two circumstances may be the cause of the important difference observed between the models fitting to data corresponding to 463 K runs and to data corresponding to the rest of temperatures: (1) a temperature increase may lead to a change of the rate limiting step, thus a change of the kinetic model and/or (2) the considerable amount of water produced in experiments carried out at high temperatures (at 463 K the amount of water can reach up to 0.25 molar fraction) play an important role on the catalytic reaction.

Experiments starting from 1-butanol/water and 1-butanol/DNBE mixtures.

To stress the effect of reaction products on the reaction rate and to break the constancy of the ratio a_{H2O}/a_{DNBE} a set of experiments starting from mixtures of 1-butanol/water and 1-butanol/DNBE was performed at 413, 433 and 453 K. Figure 5 shows the effect of water and DNBE on the initial reaction rate as a function of the initial amount of water and DNBE in the mixture (% w/w). In Figure 5a it can be seen that the initial reaction rate is highly sensitive to water content decreasing as the amount of water in the initial mixture increases. This trend is in

good agreement with the inhibitor character attributed to water. On the other hand, Figure 5b indicates that the effect of DNBE on the initial reaction rate is not remarkable suggesting that the adsorption of the ether may be negligible.

Besides reducing the initial reaction rate of DNBE synthesis, water also affects the catalyst selectivity. As it can be seen in Figure 6, mixtures with higher initial amount of water present, after 7 hours of experiment, lower selectivity to DNBE. The drop in DNBE selectivity is due to an increase in the formation of olefins and the secondary alcohol, however, selectivity to the branched ether, 1-(1-methylpropoxy) butane, is not affected. Water molecules adsorb preferentially on the active sites, blocking them. As the number of active sites blocked by water increases, the probability of finding two or more molecules of 1-butanol adsorbed on the catalyst surface close enough decreases reducing the extent of the bimolecular dehydration of 1-butanol and enhancing the intramolecular dehydration to yield the olefin 1-butene. Data of 0 corresponds to experiments performed at 453 K. For lower temperatures (413 and 433 K) the amount of water in the initial mixture does not have a significant effect on the products distribution which may be due to the fact that the intramolecular dehydration of 1-butanol to 1-butene is enhanced at high temperatures. The presence of DNBE in the starting mixture does not have any significant effect on the product distribution either.

General (Table 3) and simplified models (see Supplementary Data) were fitted to data corresponding to experiments starting from mixtures of 1-butanol/water and 1-butanol/DNBE. Data of experiments performed with pure 1-butanol were not included in this analysis with the aim of facilitate differentiation among models that are equivalent when the relationship between activities is almost constant. Best kinetic models are gathered in Table 5. As it can be seen, the fact of breaking the constancy of a_{H2O}/a_{DNBE} makes possible to differentiate between models that in the previous set of experiments (pure 1-butanol) were equivalent. In contrast to results gathered in Table 4, the model which stems from a LHHW formalism where the desorption of water is considered de rate limiting step and assuming the amount of free active sites negligible (LHHW-RLS4/1b, see Equation 13) does not fit satisfactorily experimental data (with SSRE higher than 20). Nevertheless, the LHHW model where the rate limiting steps is considered to

be the desorption of DNBE (LHHW-RLS3/1b, see Equation 14) still does. LHHW models obtained assuming that the surface reaction is the rate limiting step, LHHW-RLS2/1b (Equation 15) (considering the amount of free active sites negligible) and LHHW-RLS2/3b (Equation 16) (considering negligible both the amount of free active sites and the adsorption of DNBE) with n = 0, 1 and 2 also fit adequately data (except for LHHW-RLS2/3b with n = 2 where the SSRE is 2.36) however, uncertainty of parameters corresponding to model LHHW-RLS2/1b with n = 0 and 1 is significant. It should be noted that all these models (Table 5) include in their denominator the term of water adsorption.

Figure 7 shows the comparison between the calculated and experimental reaction rates, as well as the residual distribution, for the two models of Table 5 which present the lowest SSRE (LHHW-RLS3/1b and LHHW-RLS2/1b with n = 2). As it can be seen, the model LHHW-RLS3/1b (Figures 7a and c) fits the experimental data satisfactorily with a random distribution of residuals. However, in Figure 7b it can be observed that, at 453 K, model LHHW-RLS2/1b with n = 2 overestimates low and high values of reaction rates and, on the other hand, underestimates medium values of reaction rates. Consequently, the residuals do not shown a completely random distribution (Figure 7d).

Apparent activation energies computed by models LHHW-RLS3/1b and LHHW-RLS2/1b from experiments starting from mixtures of 1-butanol/water and 1-butanol/DNBE (Table 5) are slightly higher than values computed by the same model but from experiments starting from pure 1-butanol (Table 4). This fact is in agreement with the inhibiting effect attributed to water.[13-16] In the next section, general and simplified kinetic models where modified in order to directly introduce the inhibiting effect of water.

Modified kinetic models

Several authors have reported the strong inhibition effect of water in reactions carried out over ion exchange resins[13-16]. In those works, water is considered to adsorb preferentially on the sulfonic groups, blocking the adsorption of reactants and thus, suppressing the catalytic reaction. The common approach to model the water inhibition effect is to modify the rate

constant in such a way that only the fraction of available active sites (not blocked by water molecules, 1- θ_{H2O}) are taken into account. The fraction of acid sites blocked by water molecules (θ_{H2O}) can be expressed by an adsorption isotherm. In Table 6 three correction factors derived from Langmuir (Equations 18 and 19) and Freundlich (Equation 17) adsorption isotherms are shown. In these expressions *m* is the total number of active sites taking part in the rate-limiting step.

Three new sets of models were obtained by adding the three correction factors gathered in Table 6 to both the general kinetic models (Table 3) and the simplified kinetic models (Supplementary Data section). In all the cases the variation of K_w with temperature was supposed to be:

$$K_w = \exp\left[K_{w_1} - K_{w_2} \left(\frac{1}{T} - \frac{1}{T_{ref}} \right) \right] \qquad (20)$$

Modified models were fitted to experimental data. The fact of adding the correction factors defined by Equations 18 and 19 did not improve the fittings. However, the correction factor derived from the Freundlich adsorption isotherm (Equation 17) provides important improvements.

For experiments starting from pure 1-butanol, modified models (including the Freundlich correction factor) that best fit rate date are the same as those obtained when the correction factor was not included (Table 4) but eliminating the term of water adsorption from the denominator of Equations 14 and 15 (or, given the equivalence between models due to the constancy of the ratio a_{H2O}/a_{DNBE}, the term of DNBE adsorption in the denominator of Equations 13 and 15). Models with the Freundlich correction factor present lower SSRE (mainly due to an improvement of the fitting to data corresponding to experiments carried out at 463 K); however, the uncertainty of the fitted parameter is higher.

When models including the Freundlich correction factor were fitted to rate data corresponding to experiments starting from mixtures 1-butanol/products, in contrast to the results obtained in the fitting of the models without correction factor (Table 5), modified models that do not include a water adsorption term in the denominator (LHHW-RLS2/2b, Equation 21,

and LHHW-RLS4/2b, Equation 22) are the ones that best fit the experimental data (see Table 7). Model LHHW-RLS4/2b stems from a LHHW formalism where the desorption of water is considered the RLS and assuming negligible the amount of free active sites and the adsorption of DNBE. Model LHHW-RLS2/2b stems from a LHHW formalism where the RLS is the surface reaction and considering the amount of free active sites and the adsorption of water negligible. Furthermore, model LHHW-RLS2/1b also has very low values of SSRE but the uncertainty of the parameters is higher.

From the results gathered in Table 5 and Table 7 it can be concluded that water effect must be included in the model either by means of the Freundlich correction factor (i.e., considering that water molecules block the active sites reducing the number of available ones), or in the adsorption term. Nevertheless, including the Freundlich correction factor gives better results because not only reduces the SSRE but also achieve a better residual distribution (models in which the Freundlich correction factor is not included show higher residuals in experiments performed at higher temperatures). Taking into account both approach simultaneously does not improve the fitting and besides introduces more parameters to the models.

These conclusions agree with the results obtained in the set of experiments starting from pure 1-butanol (both, when the Freundlich factor is included and when is not). Thus, we can conclude that the models that best fit the experimental data (for the whole range of water activities and temperatures explored) are:

$$r = \frac{\hat{k}\cdot\frac{K_{BuOH}^{2}}{K_{BuOH}^{2+n}}\left(a_{BuOH}^{2}-\frac{a_{DNBE}\cdot a_{H_2O}}{K_{eq}}\right)}{\left(a_{BuOH}+\frac{K_{DNBE}}{K_{BuOH}}\cdot a_{DNBE}\right)^{2+n}}\left(1-K_w a_{H_2O}^{1/\alpha}\right) \qquad (21)$$

$$r = \frac{\frac{k_{H_2O}}{K_{H_2O}}\left(K_{eq}\frac{a_{BuOH}^{2}}{a_{DNBE}}-a_{H_2O}\right)}{\frac{K_{BuOH}}{K_{H_2O}}\cdot a_{BuOH}+K_{eq}\frac{a_{BuOH}^{2}}{a_{DNBE}}}\left(1-K_w a_{H_2O}^{1/\alpha}\right) \qquad (22)$$

With $\alpha = K_\alpha / T$

Equation 21 stems from a LHHW formalism in which two adjacent adsorbed molecules of 1-butanol (from the results it is difficult to distinguish the number of additional active sites - 0, 1 or 2 - that participate in the surface reaction) react to yield ether and water, being the surface reaction the rate limiting step. The formed water remains in the catalyst surface blocking the active centers. Equation 21 assumes that the number of unoccupied sites is not significant compared with occupied ones and that the adsorption of water is negligible. Equation 22 stems from a mechanism in which the rate limiting step is the desorption of water and where the adsorption of DNBE is comparatively negligible (which agrees with the fact that adding DNBE to the reaction medium does not influence the reaction rate, Figure 5) and the number of unoccupied sites is not significant. From Equation 22 it is not possible to discern if the mechanism corresponds to a LHHW formalism or to a ER-H_2O formalism as both lead to the same form of the rate equation (see in the Supplementary Data Section the models LHHW-RLS4/2b and ER_{H2O}-RLS3/1b).

General kinetic model

With the aim of finding a set of parameters that represent a wider range of activities, equations 21 and 22 were fitted to all the experimental data simultaneously. Results are gathered in Table 8.

In Figure 8a and b the reaction rate of DNBE formation estimated by models LHHW-RLS2/2b (Equation 21) and LHHW-RLS4/2b (Equation 22) including the Freundlich correction factor is compared with the experimental one. As it can be seen, both fittings are very similar. Figure 8c and d show the residual distribution for the two models.

Figure 9 plots the values of the Freundlich correction factor, $1\text{-}K_w a_{H_2O}^{1/\alpha}$, as used in models LHHW-RLS2/2b and LHHW-RLS4/2b (Table 8), versus a_{H2O} for all the temperatures tested. In both models the correction factor decreases on increasing a_{H2O} (linearly in model LHHW-RLS2/2b and sharply for low values of water activity and more moderately for higher water activities in model LHHW-RLS4/2b) and seems to be independent on the operating temperature

(which explains the high uncertainty associated with the parameter K_{w2}, see Table 8, indicating little sensitivity to this parameter in the fit).

Similar values of apparent activation energies (Table 8) were found for all the models (≈ 122 ± 2 kJ/mol). This value is slightly higher than those reported for the dehydration reactions over Amberlyst-70 of 1-pentanol to di-n-pentyl ether[20] (114.0±0.1 kJ/mol) and 1-octanol to di-n-octyl ether[21] (110±5 kJ/mol) and very similar to that reported for the dehydration of 1-hexanol to di-n-hexyl ether[35] (121 ±3 kJ/mol). Regarding the molar adsorption enthalpy differences, it is possible to see that adsorption of 1-butanol is stronger (more exothermic) than that of DNBE (models LHHW-RLS2/2b) but weaker than that of water (model LHHW-RLS4/2b). For model LHHW-RLS2/2b, the positive value of the difference between the free energy change for DNBE adsorption (ΔG_{DNBE}) and the free energy change for 1-butanol adsorption (ΔG_{BuOH}), calculated as $\left(\Delta G_{DNBE}-\Delta G_{BuOH}\right)=\left(\Delta H_{DNBE}-\Delta H_{BuOH}\right)-T\left(\Delta S_{DNBE}-\Delta S_{BuOH}\right)$, indicates that ΔG_{BuOH} is more negative than ΔG_{DNBE}, being the 1-butanol adsorption a more favored process than DNBE adsorption. In a similar way, for model LHHW-RLS4/2b, the positive value of $\left(\Delta G_{BuOH}-\Delta G_{H_2O}\right)$ indicates that the adsorption of water over the catalyst is a more favored process than 1-butanol adsorption. This trend is in agreement with the polarity of the compounds and the high water affinity of the resin.

Conclusions

The reaction rate of 1-butanol dehydration to di-n-butyl ether was found to be very sensitive to temperature and to water presence. Two kinetic models are proposed to explain the dehydration of 1-butanol to di-n-butyl ether over Amberlyst 70. One of them stems from a LHHW formalism in which two adjacent adsorbed molecules of 1-butanol react to yield ether and water, being the reversible surface reaction the rate limiting step and where the adsorption of water is negligible. The other one stems from a mechanism in which the rate limiting step is the desorption of water and where the adsorption of DNBE is negligible. The two models present several characteristics in common: (1) the strong inhibiting effect of water is taken into

account by means of a correction factor derived from a Freundlich adsorption isotherm (water is not included in the adsorption term); (2) the number of free active sites is found to be negligible compared to the occupied ones; (3) both models present similar values of SSRE and apparent activation energies (122 ± 2 kJ/mol).

Notation

A	Preexponential factor
a_j	Activity of compound *j*
ABE	Acetone-Butanol-Ethanol
BuOH	1-Butanol
DNBE	Di-n-butyl ether
d_p	Catalyst particle size
E_A	Activation Energy
ER	Eley-Rideal
ER_{DNBE}	Eley Rideal formalism where DNBE remains adsorbed
ER_{H2O}	Eley Rideal formalism where H_2O remains adsorbed
F_0	Test estatistic
$F_{distribution}$	Value of the continuous probability distribution
K_α	Freundlich parameter
$\hat{k}$	Forward rate constant for the surface reaction
K_{eq}	Equilibrium constant of DNBE formation reaction
k_j	Adsorption rate constant of compound *j*
K_j	Adsorption equilibrium constant of compound *j*
K_s	Surface reaction equilibrium constant
k_w	Water correction factor
k_{w1}	First parameter of the water correction factor
k_{w2}	Second parameter of the water correction factor

LHHW	Langmuir-Hinselwood- Hougen-Watson
m	Number of total active sites participating in the surface reaction
N	Stirring speed
n	Number of additional active sites participating in the surface reaction
n_{DNBE}	Moles of DNBE
R	Ideal gas constant
R^2_{adj}	Goodness of the fit
r_{cal}	Estimated reaction rate
r_{exp}	Experimental reaction rate
RLS	Rate limiting step
r_{DNBE}	Reaction rate of DNBE formation
r^0_{DNBE}	Initial reaction rate of DNBE formation
S-DVB	Styrene-divinylbenzene
s^2_E	Variance due to the experimental error
s^2_{LOF}	Variance due to the lack of fit
s^2_{PE}	Variance due to pure error
s^2_R	Variance due to the regression
SSRE	Sum of squared relative errors
t	Time
T	Temperature
T_{ref}	Midpoint T value of the analyzed range of temperatures
TCD	Thermal conductivity detector
W_{cat}	Mass of loaded catalyst
X_{BuOH}	1-Butanol conversion
Greek symbols	
α	Freundlich constant
β_i	Parameter *i*

ε_i	Uncertainty of parameter *i*
Δ	Parameters uncertainty
ΔG_j	Adsorption free energy of compound *j*
ΔH_j	Adsorption enthalpy of compound *j*
ΔS_j	Adsorption entropy of compound *j*
θ_{H2O}	Fraction of acid sites blocked by water molecules
σ	Active site

1 **References**

1. Mascal M. Chemicals from biobutanol: technologies and markets. *Biofuel Bioprod Bioref*. 2012;6:483-493.

2. Harvey BG, Meylemans HA. The role of butanol in the development of sustainable fuel technologies. *J Chem Technol Biotechnol.* 2010;86:2–9.

3. Cai L, Sudholt A, Lee DJ, Egolfopoulos FN, Pitsch H, Westbrook CK, Sarathy SM. Chemical kinetic study of a novel lignocellulosic biofuel: di-n-butyl ether oxidation in a laminar flow reactor and flames. *Combus Flame*. 2014;161:798–809.

4. Cascone R. Biobutanol – A replacement for bioethanol? *Chem Eng Pro*. 2008;104(8):S4 – S9.

5. Qureshi N, Ezeji TC. Butanol, 'a superior biofuel' production from agricultural residues (renewable biomass): recent progress in technology. *Biofuels, Bioprod Bioref*. 2008;2:319-330.

6. European biofuels technology platform. http://www.biofuelstp.eu/butanol.html (accessed April 2015)

7. Starkey LS. *Introduction to strategies for organic synthesis* (2nd edition). New Jersey: John Wiley & Sons, Inc., 2012.

8. Sheldon RA, van Bekkum H. *Fine Chemical through Heterogeneous Catalysis*. Weinheim (Germany):Wiley-VCH, 2001.

9. Pérez MA, Bringué R, Iborra M, Tejero J, Cunill F. Ion exchange resins as catalysts for the liquid-phase dehydration of 1-butanol to di-n-butyl ether. *Appl Catal, A*. 2014;482:38–48.

10. Olaofe O, Yue PL, Kinetics of dehydration of 1-butanol over zeolites. *Collect Czech Chem Commun.* 1985;501:1784-1800.

11. Krampera F, Beránek L. Kinetics of individual reactions in reaction network 1-butanol-di-(1-butyl) ether-butenes-water on alumina. *Collect Czech Chem Commun.*1986;51:774-785.

12. Sow B, Hamoudi S, Zahedi-Niaki MH, Kaliaguine S. 1-Butanol etherification over sulfonated mesostructured silica and organo-silica. *Microporous Mesoporous Mater*. 2005;79:129–136

13. Gates BC, Rodriguez W. General and specific acid catalysis in sulfonic acid resins. *J Catal.* 1973;31:27-31.

14. du Toit E, Nicol W. The rate inhibiting effect of water as a product on reactions catalyzed by cation exchange resins: formation of mesityl oxide from acetone as case study. *App Catal, A.* 2004;277:219-225.

15. Limbeck U, Altwicker C, Kunz U, Hoffmann U. Rate expression for THF synthesis on acidic ion exchange resin. *Chem Eng Sci*. 2001;56:2171-2178.

16. Yang BL, Maeda M, Goto S. Kinetics of liquid phase synthesis of tert-amyl methyl ether from tert-amyl alcohol and methanol catalyzed by ion exchange resin. *J Chem Kinet*. 1997;30:137-143.

17. Fisher S, Kunin R. Routine Exchange Capacity Determinations of Ion Exchange Resins. *J Anal Chem.* 1955;27:1191-1194.

18. Guilera J, Bringué R, Ramírez E, Iborra M, Tejero J. Synthesis of ethyl octyl ether from diethyl carbonate and 1-octanol over solid catalysts. A screening study. *Appl Catal, A.* 2012;413– 414:21– 29.

19. Box GEP, Hunter JS, Hunter WH. Statistics for experimenters. *Design, Innovation and Discovery* (2nd edition). New Jersey: John Wiley & Sons Inc., 2005.

20. Bringué R, Ramírez E, Fité C, Iborra M, Tejero J. Kinetics of 1-pentanol etherification without water removal. *Ind Eng Chem Res*. 2011;50:7911-7919.

21. Casas C. Synthesis of C_{10}-C_{16} linear symmetrical ethers from n-alcohols over heterogeneous acid catalysts. PhD Thesis. University of Barcelona, 2013.

22. Montgomery DC. *Fitting regression models. Design and Analysis of Experiments* (5th edition). John Wiley & Sons Inc., 2001.

23. Pérez-Maciá MA, Bringué R, Iborra M, Tejero J, Cunill F. Thermodynamic equilibrium for the dehydration of 1-butanol to di-n-butyl ether. *Chem Eng Res Des*. 2015;102:186–195.

24. Hill CG Jr. *Elements of heterogeneous catalysis. An introduction to chemical engineering kinetics & reaction design*. John Wiley & Sons, Inc., 1977.

25. Yang KH, Hougen OA. Determination of mechanisms of catalyzed gaseous reactions. *Chem Eng Prog*. 1950;46 (3):146-157.

26. Levenberg K. A Method for the Solution of Certain Problems in Least Squares. *Quart Appl Math.* 1944;2:64–168.

27. Marquardt D. An Algorithm for Least-Squares Estimation of Nonlinear Parameters. *SIAM J Appl Math.* 1963;11:431–441.

28. Park H, Stefanski LA. Relative-error prediction. *Statist Probab Lett*. 1998;40:227-236.

29. Tofallis C. Least Squares Percentage Regression. *J Mod App Stat Meth*. 2008;7 (2):526-534.

30. Kittrell JR. Mathematical modeling of chemical reactions. *Adv Chem Eng*. 1970;8:97–183.

31. Weidlicht U, Gmehling J. A modified UNIFAC model. 1. Prediction of VLE, hE, and $\gamma\infty$. *Ind Eng Chem Res*. 1987;26 (7):1372-1381.

32. Gmehling J, Li J, Schiller M. A modified UNIFAC model. 2. Present parameter matrix and results for different thermodynamic properties. *Ind Eng Chem Res*. 1993;32:178-193.

33. Gmehling J, Lohmann J, Jakob A, Li J, Joh R. A modified UNIFAC (Dortmund) model. 3. Revision and extension. *Ind Eng Chem Res.* 1998;37:4876-4882.

34. Jakob A, Grensemann H, Lohmann J, Gmehling J. Further development of modified UNIFAC (Dortmund): revision and extension 5. *Ind Eng Chem Res.* 2006;45:7924-7933.

35. Bringué R, Ramírez E, Iborra M, Tejero J, Cunill F. Kinetics of 1-hexanol etherification on Amberlyst 70. *Chem Eng J*. 2014;246:71–78.

CAPTIONS TO FIGURES

Figure 1. (a) 1-butanol conversion, (b) selectivity to DNBE and (c) reaction rate of DNBE synthesis as a function of temperature: (■) 413 K; (○) 423 K; (♦) 433 K; (Δ) 443 K; (●) 453 K; (□) 463 K. Experiments starting from pure 1-butanol, 1 g of catalyst, d_p = 0.4 – 0.63 mm, 4 MPa, 500 rpm. The error bars indicate the confidence interval at a 95% probability level. Most error bars are smaller than markers.

Figure 2. Reaction rate of DNBE synthesis as a function of (a) 1-butanol activity; (b) water activity; (c) DNBE activity. (■) 413 K, (○) 423 K, (♦) 433 K, (Δ) 443 K, (●) 453 K, (□) 463 K. Experiments starting from pure 1-butanol, 1 g of catalyst, d_p = 0.4 – 0.63 mm, 4 MPa, 500 rpm.

Figure 3. Evolution of the ratio a_{H2O}/a_{DNBE} with time for experiments starting from pure 1-butanol. (■) 413 K, (○) 423 K, (♦) 433 K, (Δ) 443 K, (●) 453 K, (□) 463 K. Experiments starting from pure 1-butanol, 1 g of catalyst, d_p = 0.4 – 0.63 mm, 4 MPa, 500 rpm.

Figure 4. (a) Calculated reaction rates by model LHHW-RLS4/1b (Equation 13) versus experimental rates; (b) residuals distribution. (■) 413 K, (○) 423 K, (♦) 433 K, (Δ) 443 K, (●) 453 K, (□) 463 K. Experiments starting from pure 1-butanol, 1 g of catalyst, d_p = 0.4 – 0.63 mm, 4 MPa, 500 rpm.

Figure 5. Influence of (a) water and (b) DNBE on the initial reaction rate of DNBE formation. (■) 413 K, (♦) 433 K, (●) 453 K, 1 g of catalyst, d_p = 0.4 – 0.63 mm, 4 MPa, 500 rpm.

Figure 6. Selectivity to products after 7 h reaction as a function of initial water content. T = 463 K, 1 g of catalyst, d_p = 0.4 – 0.63 mm, 4 MPa, 500 rpm. (■) DNBE, (○) 1-butene, (♦) 2-butanol, (▲) cis-2-butene, (●) trans-2-butene, (□) 1-(1-methylpropoxy) butane.

Figure 7. Calculated reaction rates by models (a) LHHW-RLS3/1b (Equation 14) and (b) LHHW-RLS2/1b with *n* = 2 (Equation 15) versus experimental rates; residuals distribution for models (c) LHHW-RLS3/1b and (d) LHHW-RLS2/1b with *n* = 2. (■) 413 K, (♦) 433 K, (○) 453 K. Experiments starting from mixtures 1-butanol/water and 1-butanol/DNBE, 1 g of catalyst, d_p = 0.4 – 0.63 mm, 4 MPa, 500 rpm.

Figure 8. Calculated reaction rates by the *modified* models (a) LHHW-RLS2/2b (Equation 21) and (b) LHHW-RLS4/2b (Equation 22) versus experimental rates; residuals distribution for models LHHW-RLS4/2b (c) and LHHW-RLS2/2b (d). (■) 413 K, (○) 423 K, (♦) 433 K, (Δ) 443 K, (●) 453 K, (□) 463 K. Rate data corresponding to all the experiments, 1 g of catalyst, d_p = 0.4 – 0.63 mm, 4 MPa, 500 rpm.

Figure 9. Freundlich factor corresponding to models LHHW-RLS2/2b (a) and LHHW-RLS4/2b (b) vs. a_{H2O} at different temperatures. (■) 413 K, (○) 423 K, (♦) 433 K, (Δ) 443 K, (●) 453 K, (□) 463 K. All the experiments, 1 g of catalyst, d_p = 0.4 – 0.63 mm, 4 MPa, 500 rpm.

Table 1. Properties of Amberlyst 70.

Catalyst	Amberlyst 70
Structure	Macroreticular
Divinylbenzene (%)	7-8
Chlorinated	Yes
Skeletal density[a] (kg/m^3)	1514
Sulfonation type	Monosulfonated
Acidity[b] (mol H^+/kg)	2.65
T_{max} (K)	463
In Dry State	
Mean particle diameter[c], d_p (mm)	0.55
Surface area[d] (m^2/g)	0.02
In Water Swollen State	
d_p[c] (mm)	0.78
Surface area[e] (m^2/g)	176
In 1-Butanol Swollen State	
d_p[c] (mm)	0.73

[a] Skeletal density measured by Helium displacement.

[b] Titration against standard base following the procedure described by Fisher and Kunin.[17]

[c] Determined by laser diffraction.

[d] BET (Brunauer-Emmet-Teller) surface area.

[e] Surface area determined from Inverse steric exclusion chromatography (ISEC) technique.

Table 2. Experimental design used to determine the optimum operational conditions.

Factors			Coded Factors			r^0 [mol/h·kg]
N [rpm]	$W_{cat.}$ [g]	d_p[mm]	A	B	C	
300	0.504	< 0.4	-1	-1.0	-1	147.7
700	0.502	< 0.4	1	-1.0	-1	150.4
300	2.067	< 0.4	-1	1.1	-1	163.6
300*	2.044	< 0.4	-1	1.1	-1	152.2
700	2.018	< 0.4	1	1.0	-1	161.0
300	0.53	0.63-0.8	-1	-1.0	1	142.2
300*	0.516	0.63-0.8	-1	-1.0	1	145.9
700	0.505	0.63-0.8	1	-1.0	1	147.6
300	2.023	0.63-0.8	-1	1.0	1	147.7
300*	2.024	0.63-0.8	-1	1.0	1	146.3
700	2.028	0.63-0.8	1	1.0	1	149.2
700*	2.034	0.63-0.8	1	1.0	1	149.7
500[a]	1.012	0.4-0.63	0	-0.3	0	155.2
500 [a]	1.011	0.4-0.63	0	-0.3	0	152.5
500 [a]	1.022	0.4-0.63	0	-0.3	0	153.8
500 [a]	1.001	0.4-0.63	0	-0.3	0	146.9

[a] From the four central point replicates an initial reaction rate mean value of 152.1 mol/h·kg (standard deviation = 3.7 mol/h·kg) can be obtained.

Table 3. Kinetic models with *n* additional active centers participating in the surface reaction ranging from 0 to 2

	Reaction Mechanisms		
RLS	**LHHW**	**ER with DNBE adsorption**	**ER with H_2O adsorption**
1-butanol adsorption	LHHW-RLS1	ER_{DNBE}-RLS1	ER_{H2O}-RLS1
	$r_{DNBE} = \frac{k_{BuOH}\left(a_{BuOH} - \left(\frac{a_{DNBE}\cdot a_{H_2O}}{K_{eq}}\right)^{0.5}\right)}{1 + K_{BuOH}\left(\frac{a_{DNBE}\cdot a_{H_2O}}{K_{eq}}\right)^{0.5} + K_{DNBE}\cdot a_{DNBE} + K_{H_2O}\cdot a_{H_2O}}$	$r_{DNBE} = \frac{k_{BuOH}\left(a_{BuOH} - \frac{a_{DNBE}\cdot a_{H_2O}}{K_{eq}\cdot a_{BuOH}}\right)}{1 + K_{BuOH}\cdot\left(\frac{a_{DNBE}\cdot a_{H_2O}}{K_{eq}\cdot a_{BuOH}}\right) + K_{DNBE}\cdot a_{DNBE}}$	$r_{DNBE} = \frac{k_{BuOH}\left(a_{BuOH} - \frac{a_{DNBE}\cdot a_{H_2O}}{K_{eq}\cdot a_{BuOH}}\right)}{1 + K_{BuOH}\cdot\left(\frac{a_{DNBE}\cdot a_{H_2O}}{K_{eq}\cdot a_{BuOH}}\right) + K_{H_2O}\cdot a_{H_2O}}$
Surface reaction	LHHW-RLS2	ER_{DNBE}-RLS2	ER_{H2O}-RLS2
	$r_{DNBE} = \frac{\hat{k}\cdot K_{BuOH}^2\left(a_{BuOH}^2 - \frac{a_{DNBE}\cdot a_{H_2O}}{K_{eq}}\right)}{\left(1 + K_{BuOH}\cdot a_{BuOH} + K_{DNBE}\cdot a_{DNBE} + K_{H_2O}\cdot a_{H_2O}\right)^{2+n}}$	$r_{DNBE} = \frac{\hat{k}\cdot K_{BuOH}\left(a_{BuOH}^2 - \frac{a_{DNBE}\cdot a_{H_2O}}{K_{eq}}\right)}{\left(1 + K_{BuOH}\cdot a_{BuOH} + K_{DNBE}\cdot a_{DNBE}\right)^{1+n}}$	$r_{DNBE} = \frac{\hat{k}\cdot K_{BuOH}\left(a_{BuOH}^2 - \frac{a_{DNBE}\cdot a_{H_2O}}{K_{eq}}\right)}{\left(1 + K_{BuOH}\cdot a_{BuOH} + K_{H_2O}\cdot a_{H_2O}\right)^{1+n}}$
DNBE desorption	LHHW-RLS3	ER_{DNBE}-RLS3	
	$r_{DNBE} = \frac{k_{DNBE}\left(K_{eq}\frac{a_{BuOH}^2}{a_{H_2O}} - a_{DNBE}\right)}{1 + K_{BuOH}\cdot a_{BuOH} + K_{DNBE}\cdot\left(K_{eq}\frac{a_{BuOH}^2}{a_{H_2O}}\right) + K_{H_2O}\cdot a_{H_2O}}$	$r_{DNBE} = \frac{k_{DNBE}\left(K_{eq}\frac{a_{BuOH}^2}{a_{H_2O}} - a_{DNBE}\right)}{1 + K_{BuOH}\cdot a_{BuOH} + K_{DNBE}\cdot\left(K_{eq}\frac{a_{BuOH}^2}{a_{H_2O}}\right)}$	
H_2O desorption	LHHW-RLS4		ER_{H2O}-RLS3
	$r_{DNBE} = \frac{k_{H_2O}\left(K_{eq}\frac{a_{BuOH}^2}{a_{DNBE}} - a_{H_2O}\right)}{1 + K_{BuOH}\cdot a_{BuOH} + K_{DNBE}\cdot a_{DNBE} + K_{H_2O}\cdot\left(K_{eq}\frac{a_{BuOH}^2}{a_{DNBE}}\right)}$		$r_{DNBE} = \frac{k_{H_2O}\left(K_{eq}\frac{a_{BuOH}^2}{a_{DNBE}} - a_{H_2O}\right)}{1 + K_{BuOH}\cdot a_{BuOH} + K_{H_2O}\cdot\left(K_{eq}\frac{a_{BuOH}^2}{a_{DNBE}}\right)}$

Table 4. Best kinetic models (fitted parameters, confidence interval for a 95% of probability, sum of squared relative errors and goodness of the fit) for experiments starting from pure 1-butanol.

LHHW-RLS4/1b
RLS: water desorption. Assuming the amount of free active sites to be negligible.

$$r_{DNBE} = \frac{\frac{k_{H_2O}}{K_{H_2O}}\left(K_{eq}\frac{a_{BuOH}^2}{a_{DNBE}} - a_{H_2O}\right)}{\frac{K_{BuOH}}{K_{H_2O}}\cdot a_{BuOH} + \frac{K_{DNBE}}{K_{H_2O}}\cdot a_{DNBE} + K_{eq}\frac{a_{BuOH}^2}{a_{DNBE}}} \quad (13)$$

SSRE = 0.59 R^2_{adj} **= 0.99** **Δ = 0.60**

Parameters

A	E_A [kJ/mol]	$\Delta S_{BuOH} - \Delta S_{H2O}$ [J/mol·K]	$\Delta H_{BuOH} - \Delta H_{H2O}$ [kJ/mol]	$\Delta S_{DNBE} - \Delta S_{H2O}$ [J/mol·K]	$\Delta H_{DNBE} - \Delta H_{H2O}$ [kJ/mol]
24.2±1.0	112.8±3.5	38.9±1.9	-50.7±17.8	44.8±2.8	48.0±22.7

LHHW-RLS3/1b
RLS: DNBE desorption. Assuming the amount of free active sites to be negligible.

$$r_{DNBE} = \frac{\frac{k_{DNBE}}{K_{DNBE}}\left(K_{eq}\frac{a_{BuOH}^2}{a_{H_2O}} - a_{DNBE}\right)}{\frac{K_{BuOH}}{K_{DNBE}}\cdot a_{BuOH} + K_{eq}\frac{a_{BuOH}^2}{a_{H_2O}} + \frac{K_{H_2O}}{K_{DNBE}}\cdot a_{H_2O}} \quad (14)$$

SSRE = 0.60 R^2_{adj} **= 0.99** **Δ = 0.65**

Parameters

A	E_A [kJ/mol]	$\Delta S_{BuOH} - \Delta S_{DNBE}$ [J/mol·K]	$\Delta H_{BuOH} - \Delta H_{DNBE}$ [kJ/mol]	$\Delta S_{H2O} - \Delta S_{DNBE}$ [J/mol·K]	$\Delta H_{H2O} - \Delta H_{DNBE}$ [kJ/mol]
24.7±1.1	110.7±4.0	37.3±1.3	-53.9±16.5	36.0±3.4	47.9±27.1

LHHW-RLS2/1b
RLS: surface reaction. Assuming the amount of free active sites to be negligible.

$$r_{DNBE} = \frac{\hat{k}\cdot\frac{K_{BuOH}^2}{K_{BuOH}^{2+n}}\left(a_{BuOH}^2 - \frac{a_{DNBE}\cdot a_{H_2O}}{K_{eq}}\right)}{\left(a_{BuOH} + \frac{K_{DNBE}}{K_{BuOH}}\cdot a_{DNBE} + \frac{K_{H_2O}}{K_{BuOH}}\cdot a_{H_2O}\right)^{2+n}} \quad (15)$$

n	**0**	**1**	**2**
SSRE:	**0.94**	**0.96**	**1.01**
R^2_{adj} **:**	**0.97**	**0.98**	**0.97**
Δ:	**1.79**	**1.99**	**2.59**
Parameters			
A:	25.4±1.1	25.5±1.1	25.6±1.1
E_A [kJ/mol]:	118.5±3.9	118.7±4.0	118.9±4.1
$\Delta S_{DNBE} - \Delta S_{BuOH}$ [J/mol·K]:	6.9±2.6	4.1±3.6	2.2±4.3
$\Delta H_{DNBE} - \Delta H_{BuOH}$ [kJ/mol]:	-26.3±26.4	-27.3±28.9	-28.0±29.7
$\Delta S_{H2O} - \Delta S_{BuOH}$ [J/mol·K]:	-12.8±15.3	-10.0±12.1	-8.3±9.8
$\Delta H_{H2O} - \Delta H_{BuOH}$ [kJ/mol]:	116.7±92.2	83.4±12.1	66.6±48.4

Table 5. Best kinetic models (fitted parameters, confidence interval for a 95% of probability, sum of squared relative errors and goodness of the fit) for experiments starting from mixtures 1-butanol/water and 1-butanol/DNBE.

LHHW-RLS3/1b (see Equation 14) **RLS: DNBE desorption. Assuming the amount of free active sites to be negligible.**					
SSRE = 0.36		R^2_{adj} **= 1.00**		**Δ = 2.53**	
Parameters					
A	E_A [kJ/mol]	$\Delta S_{BuOH} - \Delta S_{DNBE}$ [J/mol·K]	$\Delta H_{BuOH} - \Delta H_{DNBE}$ [kJ/mol]	$\Delta S_{H2O} - \Delta S_{DNBE}$ [J/mol·K]	$\Delta H_{H2O} - \Delta H_{DNBE}$ [kJ/mol]
14.4±0.8	117.8±6.7	33.6±1.8	-18.4±18.5	38.9±0.9	3.9±9.1

LHHW-RLS2/1b (see Equation 15) **RLS: surface reaction. Assuming the amount of free active sites to be negligible.**			
n	**0**	**1**	**2**
SSRE:	**0.52**	**0.45**	**0.43**
R^2_{adj} **:**	**0.98**	**0.98**	**0.98**
Δ:	**13.59**	**6.61**	**1.89**
Parameters			
A:	16.9 ± 1.0	16.9 ± 0.8	16.9 ± 0.8
E_A [kJ/mol]:	120.7 ± 5.8	122.7 ± 4.7	123.9 ± 4.4
$\Delta S_{DNBE} - \Delta S_{BuOH}$ [J/mol·K]:	-16.7 ± 7.9	-9.5 ± 1.9	-7.8 ± 1.1
$\Delta H_{DNBE} - \Delta H_{BuOH}$ [kJ/mol]:	-59 ± 162	3.4 ± 21.8	10.2 ± 12.0
$\Delta S_{H2O} - \Delta S_{BuOH}$ [J/mol·K]:	4.9 ± 0.5	2.0 ± 0.3	0.2 ± 0.3
$\Delta H_{H2O} - \Delta H_{BuOH}$ [kJ/mol]:	463.2 ± 6159	2.8 ± 4.3	4.0 ± 3.4

LHHW-RLS2/3b
RLS: surface reaction.
Assuming negligible the amount of free active sites and the adsorption of DNBE.

$$r_{DNBE} = \frac{\hat{k} \cdot \frac{K^2_{BuOH}}{K^{2+n}_{BuOH}} \left(a^2_{BuOH} - \frac{a_{DNBE} \cdot a_{H_2O}}{K_{eq}} \right)}{\left(a_{BuOH} + \frac{K_{H_2O}}{K_{BuOH}} \cdot a_{H_2O} \right)^{2+n}} \qquad (16)$$

n	**0**	**1**	**2**
SSRE:	**0.54**	**1.02**	
R^2_{adj} **:**	**0.98**	**0.98**	
Δ:	**2.35**	**0.70**	
Parameters			
A:	16.1 ± 0.7	14.2 ± 0.7	
E_A [kJ/mol]:	122.1 ± 5.4	125.2 ± 6.5	
$\Delta S_{H2O} - \Delta S_{BuOH}$ [J/mol·K]:	4.6 ± 0.4	1.2 ± 0.5	
$\Delta H_{H2O} - \Delta H_{BuOH}$ [kJ/mol]:	2.5 ± 6.0	10.7 ± 6.1	

Table 6. Correction factors to represent water inhibiting effect on reaction rate

Equation	Correction factor	Comments	Ref.
(17)	$\left(1 - K_w \cdot a_{H_2O}^{1/\alpha}\right)^m$ with $\alpha = K_\alpha / T$	Freundlich isotherm.	14
(18)	$\left(\frac{1}{1 + K_w \cdot a_{H_2O}}\right)^m$	Langmuir isotherm where a molecule of water adsorbs on one active site.	16
(19)	$\left(\frac{1}{1 + K_w \cdot a_{H_2O}^{0.5}}\right)^m$	Langmuir isotherm where a molecule of water adsorbs on two active sites.	15

Table 7. Best *modified* kinetic models (fitted parameters, confidence interval for a 95% of probability, sum of squared relative errors and goodness of the fit) for experiments starting from mixtures 1-butanol/water and 1-butanol/DNBE.

LHHW-RLS2/1b (see Equation 15) **RLS: surface reaction. Assuming the amount of free active sites to be negligible.**			
n	**0**	**1**	**2**
SSRE:	**0.14**	**0.15**	**0.16**
R^2_{adj} **:**	**1.00**	**1.00**	**1.00**
Δ:	**3.21**	**1.37**	**1.59**
	Parameters		
A:	16.6 ± 0.6	16.6 ± 0.6	16.6 ± 0.6
E_A [kJ/mol]:	114.6 ± 3.9	115.9 ± 3.7	116.7 ± 3.7
$\Delta S_{DNBE}-\Delta S_{BuOH}$ [J/mol·K]:	-11.4 ± 2.4	-8.3 ± 1.0	-7.1 ± 0.7
$\Delta H_{DNBE}-\Delta H_{BuOH}$ [kJ/mol]:	20.5 ± 24.7	-19.5 ± 10.8	19.0 ± 7.0
$\Delta S_{H2O}-\Delta S_{BuOH}$ [J/mol·K]:	4.0 ± 0.4	1.3 ± 0.3	-0.3 ± 0.3
$\Delta H_{H2O}-\Delta H_{BuOH}$ [kJ/mol]:	-14.3 ± 5.3	-9.4 ± 4.3	-6.4 ± 3.7
K_{w1}:	-0.19 ± 0.55	-0.64 ± 0.65	-0.99 ± 0.70
K_{w2}:	5714 ± 2112	7572 ± 2902	8670 ± 3475
K_{α}:	65.4± 26.5	88.3 ± 26.6	86.8 ± 27.6
LHHW-RLS2/2b (see Equation 21) **RLS: Surface reaction.** **Assuming negligible the amount of free active sites and the adsorption of H_2O.**			
n	**0**	**1**	**2**
SSRE:	**0.22**	**0.23**	**0.24**
R^2_{adj} **:**	**0.99**	**0.99**	**0.99**
Δ:	**0.81**	**0.53**	**0.41**
	Parameters		
A:	16.4 ± 0.8	16.3 ± 0.7	16.3 ± 0.7
E_A [kJ/mol]:	123.2 ± 2.3	123.2 ± 2.4	123.2 ± 2.5
$\Delta S_{DNBE}-\Delta S_{BuOH}$ [J/mol·K]:	-9.5 ± 1.5	-7.6 ± 0.8	-6.7 ± 0.6
$\Delta H_{DNBE}-\Delta H_{BuOH}$ [kJ/mol]:	34.0 ± 14.5	25.5 ± 8.2	22.5 ± 5.8
K_{w1}:	-0.10 ± 0.02	-0.23 ± 0.02	-0.32 ± 0.02
K_{w2}:	265 ± 166	415 ± 164	527 ± 156
K_{α}:	550.0 ± 34.8	499.6 ± 25.5	477.4 ± 21.0

LHHW-RLS4/2b (see Equation 22) **RLS: Desorption of water.** **Assuming negligible the amount of free active sites and the adsorption of DNBE.**						
SSRE = 0.25		R^2_{adj} **= 0.99**		**Δ = 1.50**		
		Parameters				
A	E_A [kJ/mol]	ΔS_{BuOH} - ΔS_{H2O} [J/mol·K]	ΔH_{BuOH} - ΔH_{H2O} [kJ/mol]	K_{w1}	K_{w2}	K_{α}
19.2±1.4	121.8±2.2	22.7±1.9	55.8±17.5	0.08±0.02	56.8±81.8	991±108

Table 8. Best *modified* kinetic models (fitted parameters, confidence interval for a 95% of probability, sum of squared relative errors and goodness of the fit) for all experimental data.

LHHW-RLS2/2b (see Equation 21) RLS: Surface reaction. Assuming negligible the amount of free active sites and the adsorption of H_2O.			
n	**0**	**1**	**2**
SSRE:	**1.24**	**1.38**	**1.50**
R^2_{adj} **:**	**0.99**	**0.99**	**0.99**
Δ:	**2.50**	**0.84**	**0.54**
	Parameters		
A:	25.4 ± 1.1	24.9 ± 1.0	24.7 ± 1.0
E_A [kJ/mol]:	121.7 ± 1.8	122.2 ± 1.9	122.6 ± 2.0
$\Delta S_{DNBE}-\Delta S_{BuOH}$ [J/mol·K]:	-9.6 ± 1.7	-7.2 ± 0.9	-6.3 ± 0.7
$\Delta H_{DNBE}-\Delta H_{BuOH}$ [kJ/mol]:	61.2 ± 12.9	42.6 ± 7.5	36.1 ± 5.4
K_{w1}:	-0.08 ± 0.03	-0.20 ± 0.03	-0.29 ± 0.02
K_{w2}:	73.3 ±180.4	233.1 ± 184.6	364.2 ± 178.6
K_{α}:	563.2 ± 42.4	499.4 ± 31.5	471.8 ± 26.2

LHHW-RLS4/2b (see Equation 22) RLS: Desorption of water. Assuming negligible the amount of free active sites and the adsorption of DNBE.						
SSRE = 1.34		R^2_{adj} **= 0.98**		**Δ = 2.54**		
			Parameters			
A	E_A [kJ/mol]	$\Delta S_{BuOH} - \Delta S_{H2O}$ [J/mol·K]	$\Delta H_{BuOH} - \Delta H_{H2O}$ [kJ/mol]	K_{w1}	K_{w2}	K_{α}
29.7±2.1	121.3±1.8	22.8±2.0	83.7±15.4	0.09±0.02	36.8±92.5	1018±128

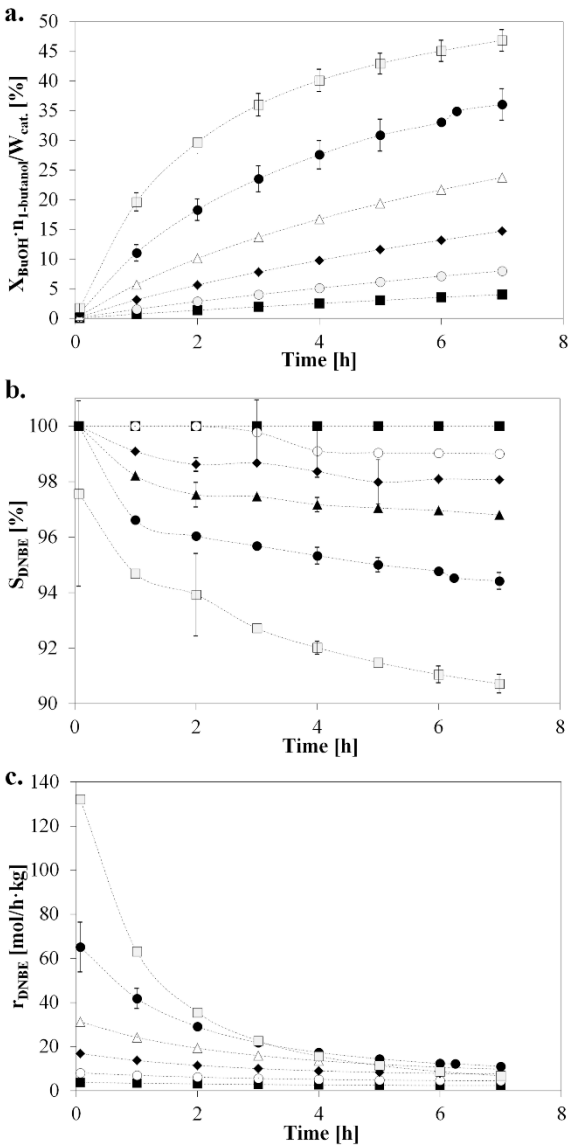

Figure 1. (a) 1-butanol conversion, (b) selectivity to DNBE and (c) reaction rate of DNBE synthesis as a function of temperature: (■) 413 K; (○) 423 K; (♦) 433 K; (Δ) 443 K; (●) 453 K; (□) 463 K. Experiments starting from pure 1-butanol, 1 g of catalyst, d_p = 0.4 – 0.63 mm, 4 MPa, 500 rpm. The error bars indicate the confidence interval at a 95% probability level. Most error bars are smaller than markers.

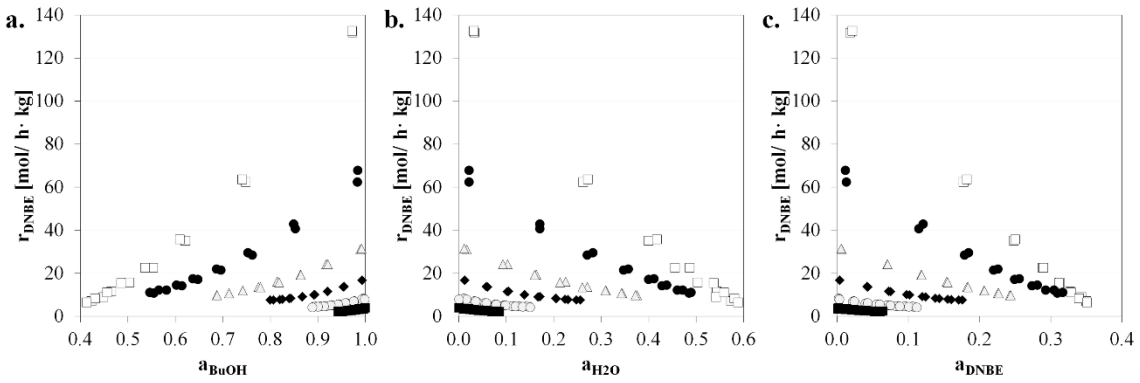

Figure 2. Reaction rate of DNBE synthesis as a function of (a) 1-butanol activity; (b) water activity; (c) DNBE activity. (■) 413 K, (○) 423 K, (♦) 433 K, (Δ) 443 K, (●) 453 K, (□) 463 K. Experiments starting from pure 1-butanol, 1 g of catalyst, d_p = 0.4 – 0.63 mm, 4 MPa, 500 rpm.

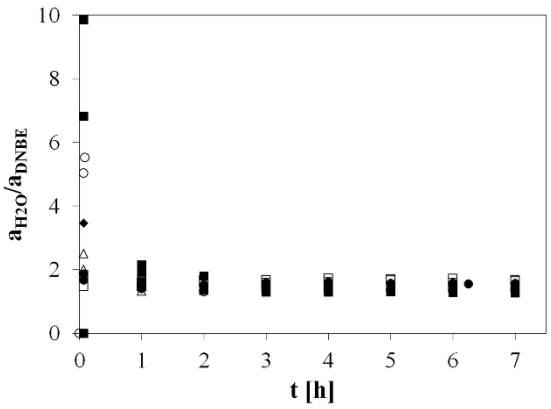

Figure 3. Evolution of the ratio a_{H2O}/a_{DNBE} with time for experiments starting from pure 1-butanol. (■) 413 K, (○) 423 K, (♦) 433 K, (Δ) 443 K, (●) 453 K, (□) 463 K. Experiments starting from pure 1-butanol, 1 g of catalyst, d_p = 0.4 – 0.63 mm, 4 MPa, 500 rpm.

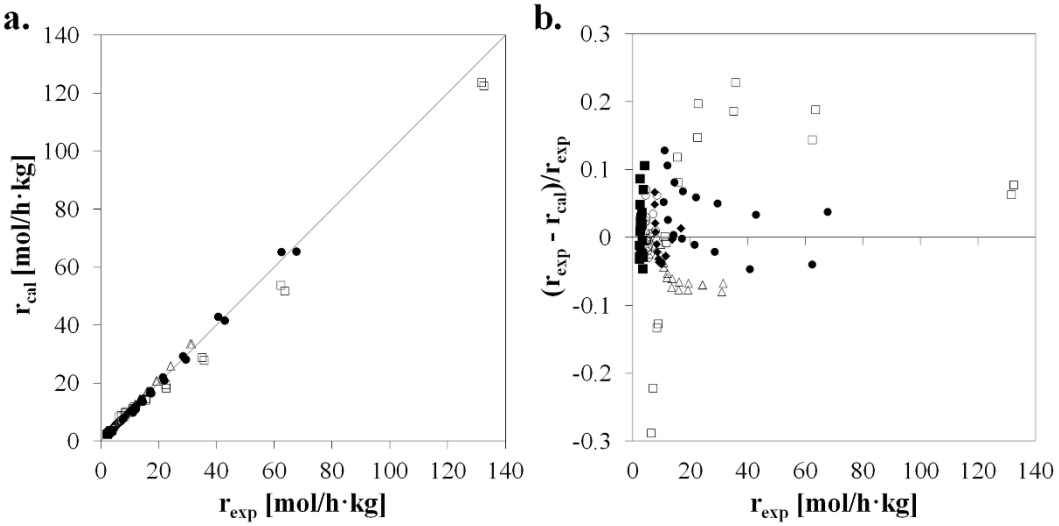

Figure 4. (a) Calculated reaction rates by model LHHW-RLS4/1b (Equation 13) versus experimental rates; (b) residuals distribution. (■) 413 K, (○) 423 K, (♦) 433 K, (Δ) 443 K, (●) 453 K, (□) 463 K. Experiments starting from pure 1-butanol, 1 g of catalyst, d_p = 0.4 – 0.63 mm, 4 MPa, 500 rpm.

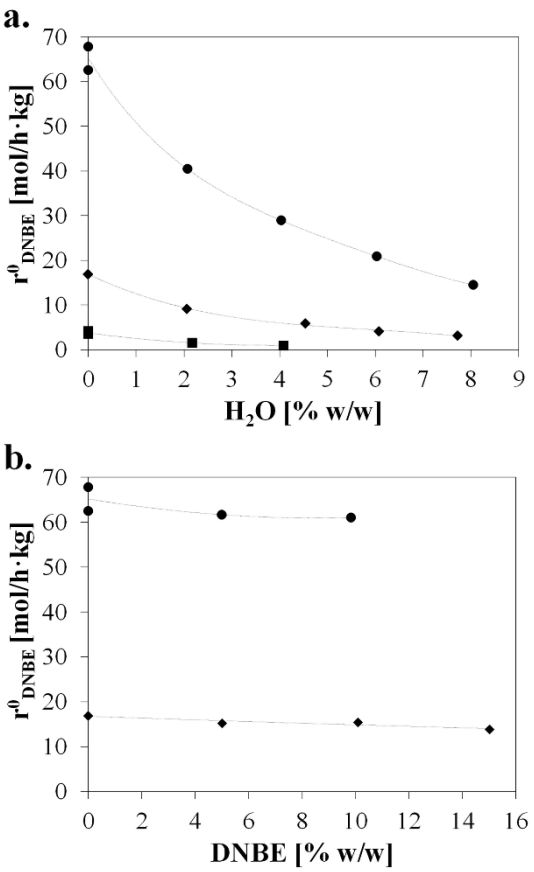

Figure 5. Influence of (a) water and (b) DNBE on the initial reaction rate of DNBE formation. (■) 413 K, (♦) 433 K, (●) 453 K, 1 g of catalyst, d_p = 0.4 – 0.63 mm, 4 MPa, 500 rpm.

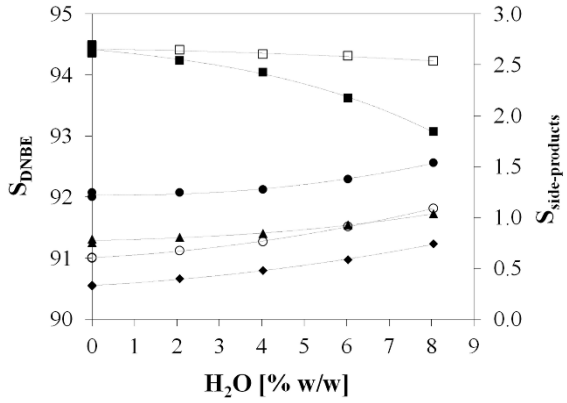

Figure 6. Selectivity to products after 7 h reaction as a function of initial water content. T = 463 K, 1 g of catalyst, d_p = 0.4 – 0.63 mm, 4 MPa, 500 rpm. (■) DNBE, (○) 1-butene, (♦) 2-butanol, (▲) cis-2-butene, (●) trans-2-butene, (□) 1-(1-methylpropoxy) butane.

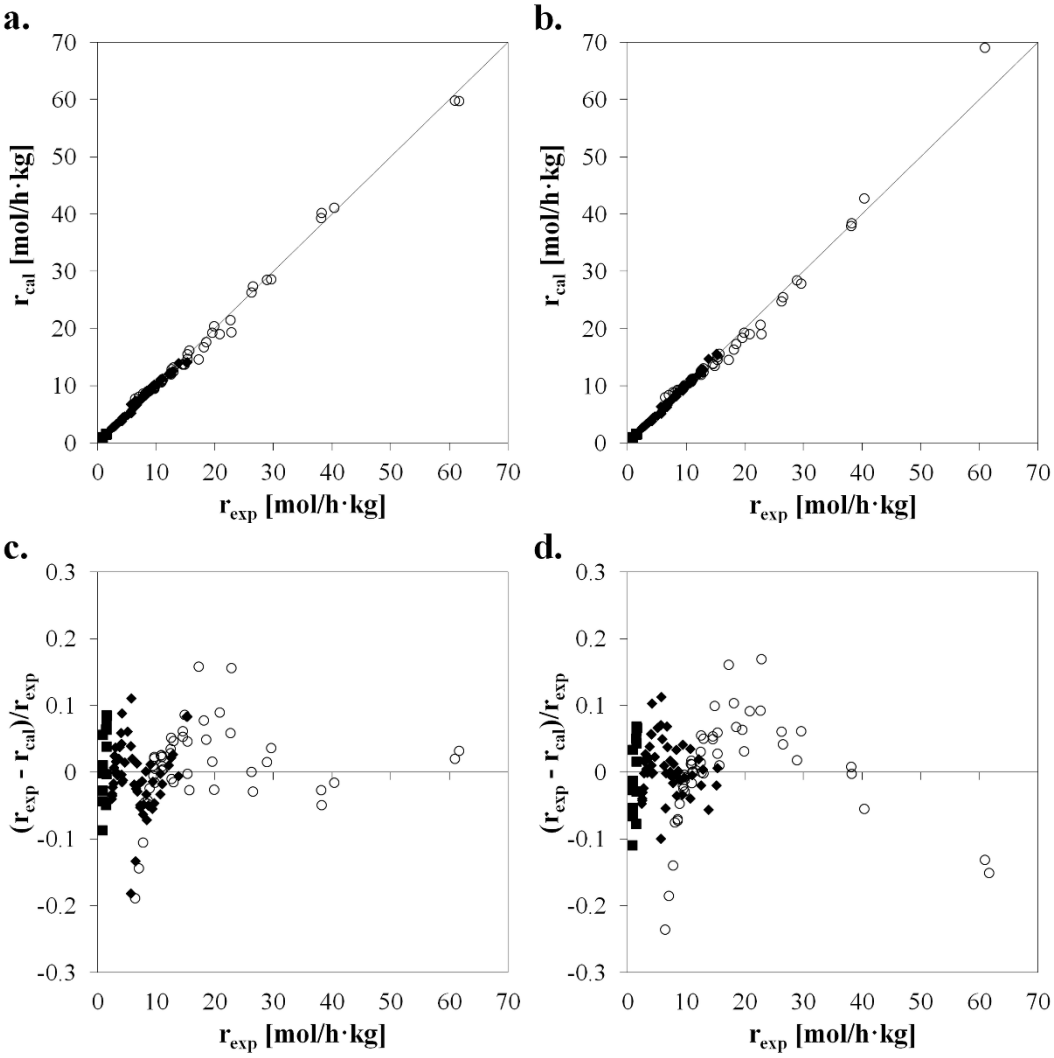

Figure 7. Calculated reaction rates by models (a) LHHW-RLS3/1b (Equation 14) and (b) LHHW-RLS2/1b with n = 2 (Equation 15) versus experimental rates; residuals distribution for models (c) LHHW-RLS3/1b and (d) LHHW-RLS2/1b with n = 2. (■) 413 K, (♦) 433 K, (○) 453 K. Experiments starting from mixtures 1-butanol/water and 1-butanol/DNBE, 1 g of catalyst, d_p = 0.4 – 0.63 mm, 4 MPa, 500 rpm

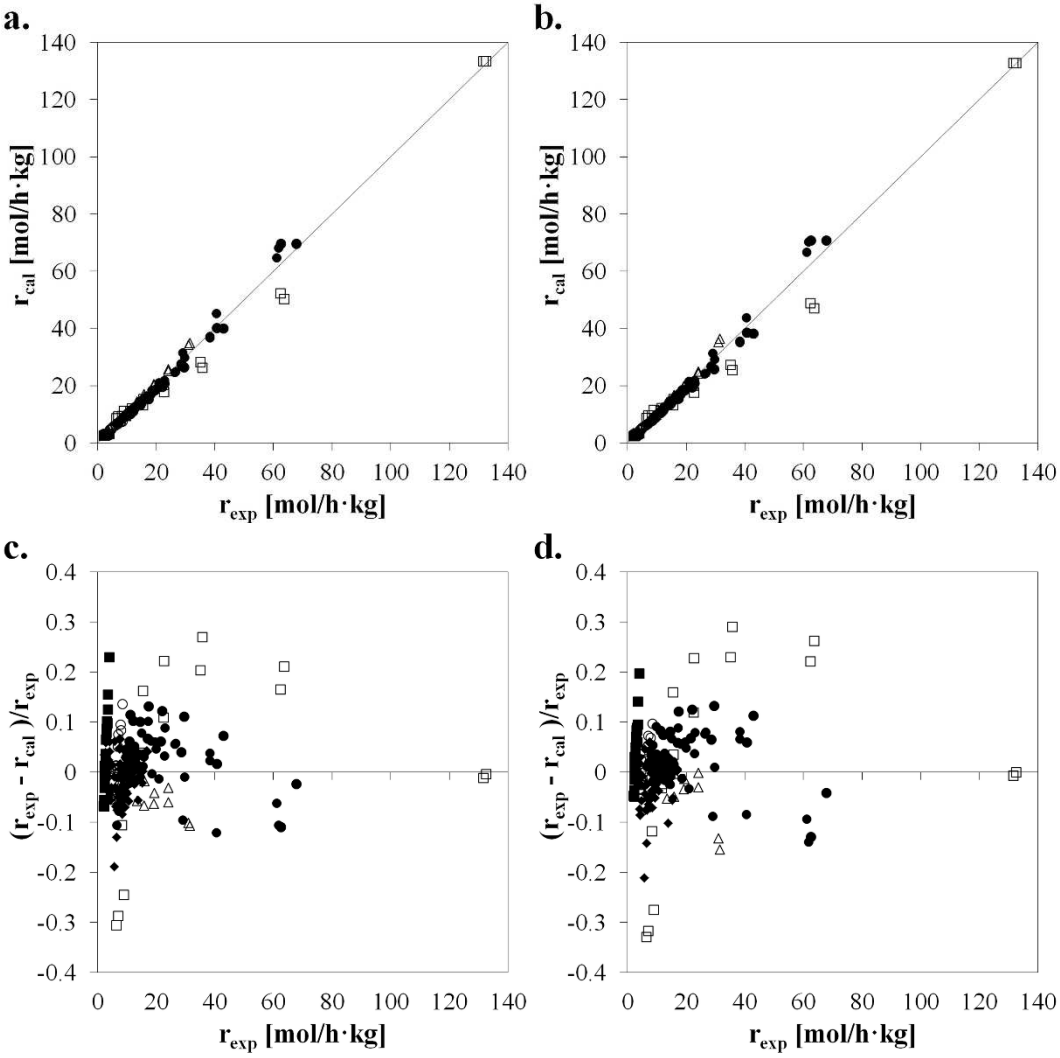

Figure 8. Calculated reaction rates by the *modified* models (a) LHHW-RLS2/2b (Equation 21) and (b) LHHW-RLS4/2b (Equation 22) versus experimental rates; residuals distribution for models LHHW-RLS4/2b (c) and LHHW-RLS2/2b (d). (■) 413 K, (○) 423 K, (♦) 433 K, (Δ) 443 K, (●) 453 K, (□) 463 K. Rate data corresponding to all the experiments, 1 g of catalyst, d_p = 0.4 – 0.63 mm, 4 MPa, 500 rpm.

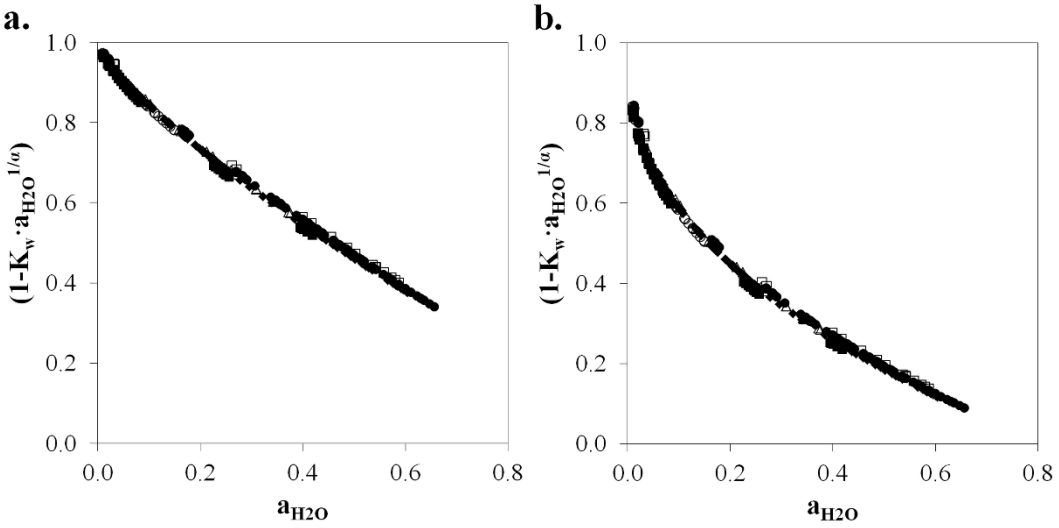

Figure 9. Freundlich factor corresponding to models LHHW-RLS2/2b (a) and LHHW-RLS4/2b (b) vs. a_{H2O} at different temperatures. (■) 413 K, (○) 423 K, (♦) 433 K, (Δ) 443 K, (●) 453 K, (□) 463 K. All the experiments, 1 g of catalyst, d_p = 0.4 – 0.63 mm, 4 MPa, 500 rpm.